Dual-Wavelength Harmonically Mode-Locked Fiber Laser With Topological Insulator Saturable Absorber

Meng Liu, Nian Zhao, Hao Liu, Xu-Wu Zheng, Ai-Ping Luo, Zhi-Chao Luo, *Member, IEEE*, Wen-Cheng Xu, Chu-Jun Zhao, Han Zhang, and Shuang-Chun Wen

***Abstract*— Dual-wavelength passively harmonic mode locking (HML) operation is demonstrated in an erbium-doped fiber laser with a microfiber-based topological insulator (TI) saturable absorber. It was found that the dual-wavelength pulse-trains possess different HML orders due to the different cavity nonlinear effects experienced by the two wavelengths. By properly adjusting the cavity parameters, dual-wavelength HML pulses with repetition rates of 388 and 239 MHz were achieved. Moreover, wavelength switchable operation of dual-wavelength HML pulses was also obtained. The experimental results reveal that the microfiber-based TI could indeed be employed as a high-performance dual-function photonic device with the saturable absorption and high nonlinear effects for the applications in fields of ultrafast and nonlinear photonics.**

***Index Terms*— Fiber lasers, topological insulator, passive mode-locking, multiwavelength.**

I. Introduction

With potential applications ranging from optical fiber sensing, optical instrumentation, optical signal processing to wavelength-division-multiplexed (WDM) fiber communication systems, multi-wavelength pulsed fiber lasers have attracted considerable attention in recent years. At present, both actively and passively mode-locked techniques have been used to achieve multi-wavelength mode-locked pulses in fiber lasers [1], [2]. Compared with the actively mode-locked techniques, multi-wavelength passively mode-locked ones could be simple, compact and low-cost since no active modulator is required in the laser cavity [3]–[5]. To date, various passive mode-locking techniques, such as the nonlinear polarization rotation (NPR) [3], nonlinear amplifying loop mirror (NALM) [4], and real saturable absorber (SA) [5], have been used to realize the multi-wavelength pulsed operation. Nevertheless, the currently reported multi-wavelength passively mode-locked fiber lasers generally deliver pulse-train with repetition rates of a few MHz.

On the other hand, high repetition rate fiber lasers have been intensively studied due to their numerous applications such as telecommunication, spectroscopy and metrology. As an alternative approach to deliver pulse-train with high repetition rate, harmonic mode locking (HML) could be employed to effectively increase the repetition rate of mode-locked pulse without decreasing cavity length [6]–[8]. Recently, it was also suggested that introducing proper high nonlinear effect into the cavity favors for the generation of HML pulses [9]. Supposing that a SA with high nonlinear effect was incorporated inside the laser cavity, both functions of SA and high nonlinear effect could be integrated into one optical device. Therefore, the generation of high-order HML pluses in a fiber laser could be achieved in a more compact design. However, all the HML fiber lasers reported so far only operated in single-wavelength regime while the multi-wavelength HML is not yet studied.

Very recently, a new type of Dirac material, similar to graphene [10]–[12], the Topological Insulators (TIs) start to be studied in fields from condensed-matter physics [13], [14] to nonlinear optics [15], [16]. Through investigating the nonlinear optical response of TIs, F. Bernard et al. found that TIs exhibit saturable absorption at telecommunication wavelengths [15]. Being different from an ordinary small-band gap material, TIs possess a small band gap in its bulk state and a gapless metallic state in its surface, which both contribute to the saturable absorption [17]. Besides that, TIs were also found to have large nonlinear refractive index with Z-scan technique [16]. Those experimental findings indicate that TIs could be potentially employed as both the SA and the high nonlinear photonic device. However, to date the TISAs are generally fabricated with a quartz plate [18]–[20] or a fiber end facet [21]–[23], which makes the interaction length between the propagation light and TIs very short. Thus, the pulse shaping affected by the nonlinear effect of TISA is less significant, where no HML operation was observed in fiber laser with a TISA.

Nevertheless, this situation could change if TIs are deposited onto a microfiber, which could effectively increase the interaction length between the light and the TIs. In this case, the nonlinear effect of the TI-based SA in fiber laser could be greatly increased, making it suitable for generating HML pulse. This concept was demonstrated recently by our group [24].

Manuscript received January 24, 2014; revised March 5, 2014; accepted March 6, 2014. Date of publication March 11, 2014; date of current version April 17, 2014. This work was supported in part by the National Natural Science Foundation of China under Grants 11074078, 61378036, 61307058, and 11304101, in part by the Ph.D. Start-Up Fund of Natural Science Foundation of Guangdong Province, China, under Grant S2013040016320, and in part by the Graduate Research and Innovation Foundation of South China Normal University, China, under Grant 2013kyjj044.

M. Liu, N. Zhao, H. Liu, X.-W. Zheng, A.-P. Luo, Z.-C. Luo, and W.-C. Xu are with the Laboratory of Nanophotonic Functional Materials and Devices, School of Information and Optoelectronic Science and Engineering, South China Normal University, Guangzhou, Guangdong 510006, China (e-mail: luoaiping@scnu.edu.cn; zcluo@scnu.edu.cn; xuwch@scnu.edu.cn).

C.-J. Zhao, H. Zhang, and S.-C. Wen are with the Key Laboratory for Micro-/Nano-Optoelectronic Devices of Ministry of Education, College of Physics and Microelectronic Science, Hunan University, Changsha 410082, China.

Color versions of one or more of the figures in this letter are available online at http://ieeexplore.ieee.org.

Digital Object Identifier 10.1109/LPT.2014.2311101

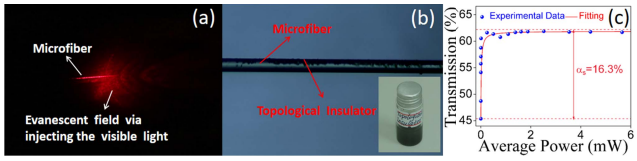

Fig. 1. (a) Evanescent field of the microfiber through launching the visible light. (b) Microscopy image of microfiber-based TISA. (c) Measured saturable absorption curve and the corresponding fitting curve.

Given that the multi-wavelength mode locking and high repetition rate pulses are of great significance in field of laser physics, it would be interesting to develop a dual-wavelength passive HML fiber laser by using a microfiber-based TISA.

In this letter, we further optimized the quality of the microfiber-based TISA by controlling the tapered fiber waist and the deposition amount of TI. The proposed TISA with ∼16.3% modulation depth and ∼38.1% non-saturable loss was obtained, which is greatly improved compared with the previous report of our group [24]. With the fabricated high-performance microfiber-based TISA, we report on the observation of dual-wavelength passively harmonic mode-locked pulses in an erbium-doped fiber (EDF) laser. Each wavelength corresponds to one sequence of pulse-train, which have different repetition rates of 388 MHz and 239 MHz. Moreover, the wavelength switchable operation can be obtained. These results further suggest that the microfiber-based TI could operate as a good candidate of saturable absorption and high nonlinear photonic device for the related applications.

II. TISA Fabrication and Characteristics

The microfibers were drawn from the standard single mode fiber by using the flame-brushing technique. In this work, the diameter of microfiber was tapered to ∼20 μm, whose insertion loss is ∼0.8 dB. Fig. 1(a) typically shows the evanescent field of the microfiber through launching the visible light. The optical force induced by the evanescent field could be used to deposit the TI onto the microfiber [25]. In our experiment, the deposition of TI on the microfiber was achieved by immersing the microfiber into the TI/acetone solution with a concentration of 0.1 mg/ml and launching a pumping light. The TI Bi_2Te_3 nano-sheets and the setup for TISA fabrication are the same as those reported in Ref. [24]. The deposition quality, such as uniformity and length, could be optimized through controlling the light power and deposition time [25]. To balance the nonlinear effect and the non-saturable loss, here the deposition length of TI was ∼0.6 mm. Fig. 1(b) shows the microscopy image of the microfiber-based TISA after evaporating at room temperature. We can see that the TI had been well deposited on the microfiber. After fabricating the TISA, its saturable absorption was measured. Using the same measurement setup with Ref. [24], the saturable absorption characteristic was shown in Fig. 1(c), in which we can see that the modulation depth is ∼16.3%, the non-saturable loss is ∼38.1% and the saturable power is ∼0.02 mW. Compared with our previous work [24], the improvement of the modulation depth and non-saturable loss could be attributed to the optimization of the deposition length of TI and the diameter of the microfiber.

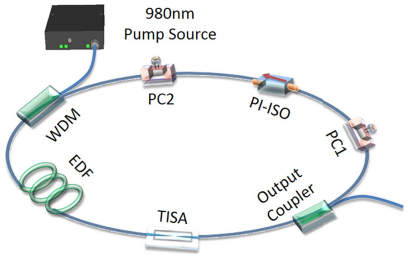

Fig. 2. Schematic of dual-wavelength passively harmonic mode-locked EDF laser with a microfiber-based TISA.

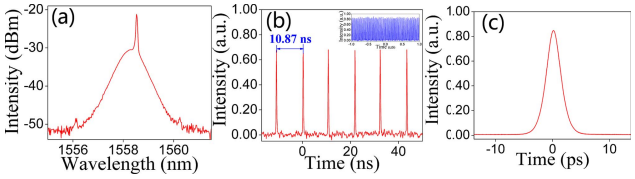

Fig. 3. Single-wavelength mode-locked operation at the repetition rate of 92 MHz. (a) Mode-locked spectrum. (b) Corresponding pulse-train. Inset: pulse-train with 2 μs span. (c) Corresponding autocorrelation trace.

III. Laser Performance and Discussion

The fabricated TISA was inserted into the laser cavity. Fig. 2 shows the schematic of the dual-wavelength passively harmonic mode-locked EDF laser with a microfiber-based TISA. The fiber laser has a ring cavity, whose cavity length is ∼40 m. Thus, the fundamental repetition rate is 5.1 MHz. A 980 nm laser diode (LD) is introduced to pump the gain fiber. A ∼5 m EDF is used to supply sufficient gain for laser emission. The polarization independent isolator (PI-ISO) is employed to ensure the unidirectional operation. Two PCs are used to adjust the polarization state of light. Taken by a 10% fiber coupler, the laser output is monitored by an optical spectrum analyzer (Anritsu MS9710C) and a 2 GHz oscilloscope (LeCroy WaveRunner 620Zi) with a 12.5 GHz high speed photodiode detector (New Focus P818-BB-35F). Moreover, the pulse profile is measured with an autocorrelator (FR-103XL).

The mode-locked operation could be easily achieved due to the saturable absorption of TI. However, because of the high nonlinear effect induced by the microfiber-based TISA, the fiber laser always tended to operate in HML state even if the pump power was low. Moreover, we also observed bunched solitons when the cavity parameters are properly adjusted. However, here we are only concerned with the HML operation. Generally, the single-wavelength mode-locked operation could be observed. Fig. 3(a) shows the optical spectrum of the single-wavelength mode-locked pulses at a pump power of 30 mW. The output spectrum is centered at 1558.3 nm with a 3-dB bandwidth of 0.9 nm. The corresponding pulse-train is presented in Fig. 3(b). Here, the repetition rate was calculated to be 92 MHz, corresponding to 18th harmonic of fundamental repetition frequency. The pulse duration was also measured, as shown in Fig. 3(c). If a sech^2 shape pulse is assumed, the pulse duration is about 3.01 ps.

As we know, squeezing the fiber in the PCs could generate polarization-dependent loss. By combining the polarization

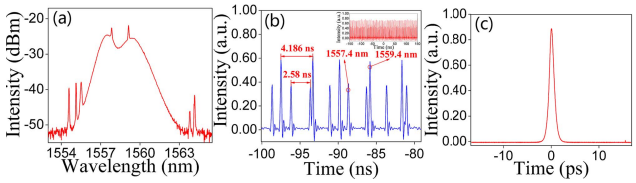

Fig. 4. Dual-wavelength HML operation. (a) Mode-locked spectrum. (b) Pulse-train. Inset: pulse-train with 600 ns span. (c) Corresponding autocorrelation trace.

dependent loss with the cavity birefringence, the spectral filter could be produced, which could be employed to achieve the multi-wavelength lasing operation [5]. Therefore, by carefully tuning the PCs, dual-wavelength HML operation was obtained. Fig. 4(a) shows the spectrum of dual-wavelength HML pulses under 116 mW pump power. The two lasing wavelengths centered at 1557.4 nm and 1559.4 nm have 3-dB bandwidths of 1.12 nm and 1.75 nm, respectively. The corresponding pulse-train is presented in Fig. 4(b). For better clarity, the pulse-train with wider scan range is also shown in the inset of Fig. 4(b). As can be seen in Fig. 4(b), it is evident that there are two sequences of pulse-trains on the oscilloscope, which have different intensities and repetition rates. It indicates that the dual-wavelength pulses operate in different harmonic numbers. By carefully analyzing the pulse-trains in Fig. 4(b), the repetition rates are 388 MHz and 239 MHz at 1557.4 nm and 1559.4 nm, respectively. In addition, the autocorrelation trace of the dual-wavelength harmonic pulse-train is shown in Fig. 4(c), whose duration is measured to be 1.3 ps. In the experimental observation, the proposed fiber laser could sustain the dual-wavelength HML operation for a long time if there were no environment perturbations applied to the laser.

To further confirm that the two sequences of pulse-trains were generated individually from the two wavelengths, a band-pass filter was used to resolve the lasing at each wavelength. Fig. 5 shows the measured results. The filtered spectra are shown in Fig. 5(a) and (b). Correspondingly, the wavelength resolved pulse-trains centered at 1557.4 nm and 1559.4 nm are presented in Fig. 5(c) and (d), respectively. In these cases, the pulse-trains measured with large scan range are also shown in the inset of Fig. 5(c) and (d). Here, the repetition rates are 388 MHz at 1557.4 nm and 239 MHz at 1559.4 nm, corresponding to the 76^{th} and 47^{th} harmonics of the fundamental repetition frequency. The measured repetition rates at both wavelengths are well consistent with those shown in Fig. 4(b), demonstrating that the two sequences of pulse-trains are indeed generated from the two wavelengths. As observed in our experiment, the pulse-trains at two wavelengths have different repetition rates. Note that the pulse durations (3-dB spectral bandwidths) and the output pulse powers at two wavelengths are not equal, resulting in the different nonlinear effects of the two pulse-trains when propagating through the TISA. It should be also noted that the harmonic number in fiber laser is related to the accumulated cavity nonlinear effect. Therefore, the different repetition rates at two wavelengths were observed. We have also shown the autocorrelation traces corresponding to the 1557.4 nm and 1559.4 nm in

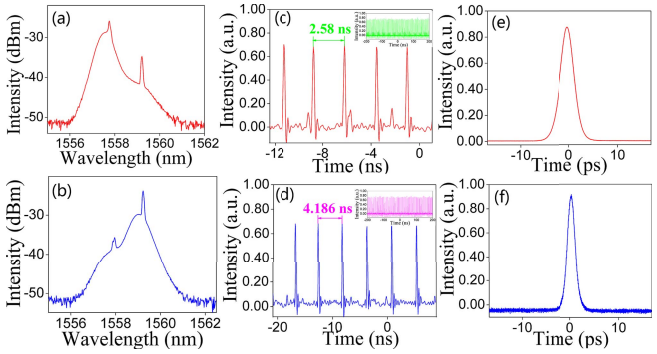

Fig. 5. Wavelength resolved dual-wavelength HML. (a) and (b) Spectra centered at 1557.4 nm and 1559.4 nm, respectively. (c) and (d) Corresponding pulse-trains. Inset: pulse-trains with large span. (e) and (f) Corresponding autocorrelation traces.

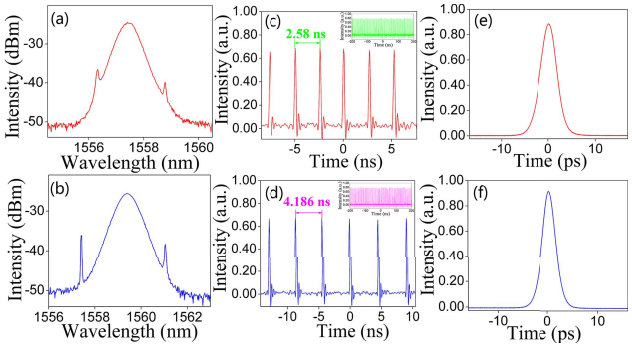

Fig. 6. Wavelength switchable operation. (a) and (b) Spectra centered at 1557.4 nm and 1559.4 nm, respectively. (c) and (d) Corresponding pulse-trains. Inset: pulse-trains with large span. (e) and (f) Autocorrelation traces.

Fig. 5(e) and (f), respectively. The pulse durations are 3.42 ps and 2.02 ps.

When the PCs were further rotated, the cavity loss for the dual-wavelength pulses could vary. If the cavity loss for one lasing wavelength is large enough while the other is sufficiently low, the wavelength switchable operation of dual-wavelength mode-locking is obtained. Fig. 6(a) and (b) show the spectra of wavelength switchable operation. In agreement with the central wavelengths of the dual-wavelength mode-locked operation, the center wavelengths of the switchable HML pulses are 1557.4 nm and 1559.4 nm, whose 3-dB bandwidths are 0.7 nm and 0.88 nm, respectively. Note that the sideband locations of mode-locked spectra varied during the wavelength switchable operation by rotating the PCs. Therefore, the spectral sidebands could be formed by four-wave-mixing effect [26]. In the time domain, Fig. 6(c) and (d) illustrate the pulse-trains centered at 1557.4 nm and 1559.4 nm, respectively, which correspond to the repetition rates of 388 MHz and 239 MHz. Note that the repetition rate of HML is dependent on the cavity loss, suggesting that the certain repetition rate could be achieved by tuning the PCs and the pump power. Therefore, the repetition rates of wavelength switchable operation could be the same as the case of dual-wavelength HML. In addition, the corresponding autocorrelation traces are shown in Fig. 6(e) and (f). The measured pulse durations are 4.09 ps and 3.17 ps at 1557.4 nm and 1559.4 nm, respectively.

In our experiment, only the dual-wavelength mode-locking operation was obtained, which could be due to the large channel spacing of the intra-cavity birefringence-induced comb filter. Therefore, in order to obtain additional mode-locked pulses, we could employ a comb filter with narrower channel spacing in the fiber laser, such as high-birefringence-based comb filter [27]. In addition, we have also investigated the laser performance of dual-wavelength HML operation at a higher pump power. However, further increasing the pump power will destroy the dual-wavelength mode-locking operation. It is probably because the variation of the pump power makes the cavity loss at a specific wavelength vary, leading to the vanishing of the dual-wavelength mode-locking state. However, it could exist in a certain range of pump power, i.e., from 53 mW to 116 mW.

IV. Conclusion

In conclusion, we have demonstrated the generation of dual-wavelength passively HML pulses in an EDF laser with a microfiber-based TISA. Using a bandpass filter, we had characterized the pulse dynamics of each individual wavelength. The repetition rates of each wavelength are 388 MHz and 239 MHz centered at 1557.4 nm and 1559.4 nm, respectively. Moreover, the wavelength switchable operation was also obtained. The experimental results further demonstrated that the microfiber-based TI could act as the high-performance photonic device with both the saturable absorption and high nonlinear effects, which will find versatile applications in fields of nonlinear and ultrafast optics.

References

[1] Y. Liu, K. S. Chiang, and P. L. Chu, "Generation of dual-wavelength picosecond pulses from a self-seeded Fabry-Perot laser diode and a polarization-maintaining fiber Bragg grating," *IEEE Photon. Technol. Lett.*, vol. 16, no. 7, pp. 1742–1744, Jul. 2004.

[2] O. G. Okhotnikov and M. Guina, "Stable single- and dual-wavelength fiber laser mode locked and spectrum shaped by a Fabry-Perot saturable absorber," *Opt. Lett.*, vol. 25, no. 22, pp. 1624–1626, Nov. 2000.

[3] Z. C. Luo *et al.*, "Tunable multiwavelength passively mode-locked fiber ring laser using intracavity birefringence-induced comb filter," *IEEE Photon. J.*, vol. 2, no. 4, pp. 571–577, Aug. 2010.

[4] L. Yun, X. M. Liu, and D. Mao, "Observation of dual-wavelength dissipative solitons in a figure-eight erbium-doped fiber laser," *Opt. Express*, vol. 20, no. 19, pp. 20992–20997, Sep. 2012.

[5] H. Zhang, D. Y. Tang, X. Wu, and L. M. Zhao, "Multi-wavelength dissipative soliton operation of an erbium-doped fiber laser," *Opt. Express*, vol. 17, no. 15, pp. 12692–12697, Jul. 2009.

[6] F. Amrani *et al.*, "Passively mode-locked erbium-doped double-clad fiber laser operating at the 322nd harmonic," *Opt. Lett.*, vol. 34, no. 14, pp. 2120–2122, Jul. 2009.

[7] G. Sobon, J. Sotor, and K. M. Abramski, "Passive harmonic mode-locking in Er-doped fiber laser based on graphene saturable absorber with repetition rates scalable to 2.22 GHz," *Appl. Phys. Lett.*, vol. 100, no. 16, pp. 161109-1–161109-4, Apr. 2012.

[8] Y. C. Meng, S. Zhang, X. Li, H. Li, J. Du, and Y. P. Hao, "Multiple-soliton dynamic patterns in a graphene mode-locked fiber laser," *Opt. Express*, vol. 20, no. 6, pp. 6685–6692, Mar. 2012.

[9] C. S. Jun, S. Y. Choi, F. Rotermund, B. Y. Kim, and D. I. Yeom, "Toward higher-order passive harmonic mode-locking of a soliton fiber laser," *Opt. Lett.*, vol. 37, no. 11, pp. 1862–1864, Jun. 2012.

[10] H. Zhang, Q. Bao, D. Tang, L. Zhao, and K. Loh, "Large energy soliton erbium-doped fiber laser with a graphene-polymer composite mode locker," *Appl. Phys. Lett.*, vol. 95, no. 14, p. 141103, Oct. 2009.

[11] Z. Sun *et al.*, "Graphene mode-locked ultrafast laser," *ACS Nano*, vol. 4, no. 2, pp. 803–810, Jan. 2010.

[12] A. Martinez and S. Yamashita, "10GHz fundamental mode fiber laser using a graphene saturable absorber," *Appl. Phys. Lett.*, vol. 101, no. 4, p. 041118, Jul. 2012.

[13] M. Z. Hasan and C. L. Kane, "Colloquium: Topological insulators," *Rev. Modern Phys.*, vol. 82, no. 4, pp. 3045–3067, Nov. 2010.

[14] X. L. Qi and S. C. Zhang, "Topological insulators and superconductors," *Rev. Modern Phys.*, vol. 83, no. 4, pp. 1057–1110, Oct. 2011.

[15] F. Bernard, H. Zhang, S. P. Gorza, and P. Emplit, "Towards mode-locked fiber laser using topological insulators," in *Nonlinear Photon., OSA Tech. Dig.*, 2012, pp. 1–3, paper NTh1A.5.

[16] S. B. Lu *et al.*, "Third order nonlinear optical property of Bi_2Se_3," *Opt. Express*, vol. 21, no. 2, pp. 2072–2082, Jan. 2013.

[17] S. Q. Chen *et al.*, "Broadband optical and microwave nonlinear response in topological insulator," *Opt. Mater. Express*, vol. 4, no. 4, pp. 587–596, Apr. 2014.

[18] C. J. Zhao *et al.*, "Ultra-short pulse generation by a topological insulator based saturable absorber," *Appl. Phys. Lett.*, vol. 101, no. 21, p. 211106, Nov. 2012.

[19] C. J. Zhao *et al.*, "Wavelength-tunable picosecond soliton fiber laser with topological insulator: Bi_2Se_3 as a mode locker," *Opt. Express*, vol. 20, no. 25, pp. 27888–27895, Dec. 2012.

[20] H. Yu *et al.*, "Topological insulator as an optical modulator for pulsed solid-state lasers," *Laser & Photon. Rev.*, vol. 7, no. 6, pp. L77–L83, Nov. 2013.

[21] Z. Q. Luo *et al.*, "1.06 μm Q-switched ytterbium-doped fiber laser using few-layer topological insulator Bi_2Se_3 as a saturable absorber," *Opt. Express*, vol. 21, no. 24, pp. 29516–29522, Dec. 2013.

[22] J. Sotor, G. Sobon, W. Macherzynski, P. Paletko, K. Grodecki, and K. M. Abramski, "Mode-locking in Er-doped fiber laser based on mechanically exfoliated Sb_2Te_3 saturable absorber," *Opt. Mater. Express*, vol. 4, no. 1, pp. 1–6, Jan. 2014.

[23] Z. Q. Luo *et al.*, "Topological-insulator passively Q-switched double-clad fiber laser at 2μm wavelength," *IEEE J. Sel. Topics Quantum Electron.*, vol. 20, no. 5, Sep./Oct. 2014, article 902708.

[24] Z. C. Luo *et al.*, "2 GHz passively harmonic mode-locked fiber laser by a microfiber-based topological insulator saturable absorber," *Opt. Lett.*, vol. 38, no. 24, pp. 5212–5215, Dec. 2013.

[25] K. Kashiwagi and S. Yamashita, "Deposition of carbon nanotubes around microfiber via evanascent light," *Opt. Express*, vol. 17, no. 20, pp. 18364–18370, Sep. 2009.

[26] H. Zhang, D. Y. Tang, L. M. Zhao, and N. Xiang, "Coherent energy exchange between components of a vector soliton in fiber lasers," *Opt. Express*, vol. 16, no. 17, pp. 12618–12623, Aug. 2008.

[27] Z. C. Luo, A. P. Luo, and W. C. Xu, "Tunable and switchable multiwavelength passively mode-locked fiber laser based on SESAM and inline birefringence comb filter," *IEEE Photon. J.*, vol. 3, no. 1, pp. 64–70, Feb. 2011.